Reconfiguration, Interrupted Aging, and Enhanced Dynamics of a Colloidal Gel Using Photoswitchable Active Doping

Mengshi Wei,[1] Matan Yah Ben Zion,[2] and Olivier Dauchot[1]
[1]Gulliver UMR CNRS 7083, ESPCI Paris, PSL Research University, 10 rue Vauquelin, 75005 Paris, France
[2]School of Physics and Astronomy, and the Center for Physics and Chemistry of Living Systems, Tel Aviv University, Tel Aviv 6997801, Israel

(Received 16 February 2023; revised 6 May 2023; accepted 1 June 2023; published 7 July 2023)

We study quasi-2D gels made of a colloidal network doped with Janus particles activated by light. Following the gel formation, we monitor both the structure and dynamics before, during, and after the activation period. Before activity is switched on, the gel is slowly aging. During the activation, the mobility of the passive particles exhibits a characteristic scale-dependent response, while the colloidal network remains connected, and the gel maintains its structural integrity. Once activity is switched off, the gel stops aging and keeps the memory of the structure inherited from the active phase. Remarkably, the motility remains larger than that of the gel, before the active period. The system has turned into a genuinely softer gel, with frozen dynamics, but with more space for thermal fluctuations. The above conclusions remain valid long after the activity period.

DOI: 10.1103/PhysRevLett.131.018301

Programmable self-assembling is a widely used bottom-up approach for achieving materials with desired properties [1–4]. A common route for self-assembly consists of engineering the intercolloid potential such that the structure, be it equilibrium or kinetically arrested, matches the expected design. The advent of active Janus colloids offers the opportunity to engineer at the local scale, not only the interactions, but also the dynamics of the self-assembling process. Such active doping has been shown both experimentally and numerically to be a realistic strategy for either driving the system toward its thermodynamically favored crystalline target structure [5–7], or modulating the structure of isotropic colloidal gels and glasses [8–12].

The case of gels is of particular interest. First, there are strong experimental evidences of anomalous mechanical responses and original dynamics in biological and reconstituted biopolymer networks [13–16]. These observations have in turn driven a large amount of theoretical work aiming at deciphering the specific microscopic mechanisms and formulating an effective medium theory [17–21]. Second, from a more fundamental perspective, gels can be seen as a prototype of slowly aging disordered out of equilibrium system, with a plethora of metastable configurations. This offers new opportunities for exploring the configuration landscape and equilibration dynamics in the presence of active dopants. As compared to glasses, gels have the advantage of presenting a structure, the descriptors of which, such as strand width, hole size, etc., are partly identified and can be monitored.

We concentrate on the simple case of colloidal gels, for which a few results have been obtained so far. It was shown experimentally that a fractal cluster colloidal gel with embedded active Janus colloids displays enhanced dynamics and a reduction in linear viscoelastic moduli in proportion to activity, while its yield stress decreases significantly even for a very small fraction of dopant [22–24]. The numerical study of the coarsening dynamics of a model colloidal gel former, including active particles, leads to the prediction of a phase diagram parametrized by the intensity and the directional persistence of the active forces [10]. When the active forces are smaller, but comparable to the interparticle attractive forces, the coarsening dynamics accelerates as activity helps drive the coalescence of the gel strands, with a strong amplification of the effect with increasing persistence. When the active forces are larger than the adhesion ones, the active colloids are no longer bound to other particles and start mediating new effective interactions among the passive particles. In the above studies the active doping is present from the early stage of gelation and therefore biases the whole gelation process, leaving aside two important questions: (i) what is the response of a passive gel with embedded Janus, yet not activated, particles to a stepwise switch of the activity? (ii) what is the fate of the gel, once the activity is switched off, after a given period of activity? This last question is of particular interest if one is to imprint permanent properties in a gel using active doping.

In this Letter, we design and study an active quasi 2D colloidal gel composed of a mixture of passive polystyrene and active Janus particles. The activity is switched on using light once the gel is formed and kept constant for a while before it is switched off. The activity level is tuned by the light intensity and kept such that the active colloids remain bounded to the gel. We monitor both the structure and dynamics before, during, and after the illumination period.

Before the activation, the gel is slowly aging. During the active phase, the mobility of the passive particles not only increases with activity, but also exhibits a characteristic scale-dependent response to activity. Our main findings concern the reconfigured gel, once activity is turned off. First, the aging is interrupted. Second, the gel keeps the memory of the structure inherited from the active phase. Third, it exhibits a *larger* mobility than that of the gel before the active period. This increase of the dynamics correlates well with the increase of softness and structural heterogeneities in the gel. Altogether, the gel has turned into a genuine different gel, the softness and mobility of which is controlled by the level of activation, and remains unaltered during several weeks.

The quasi-2D colloidal gel of thickness $h = 2.6 \pm 1.15$ μm and effective 2D packing fraction of 20% is obtained by the sedimentation of a mixture of passive $\sigma = 2$ μm diameter polystyrene particles and active 1.5 μm diameter particles, a hematite α-Fe_2O_3 cube partially protruding outside a shell of 3-methacryloxypropyltrimethoxysilane (TPM) [25–28], in the presence of polyethylene glycol (PEO with gyration ratio $R_g \simeq 25$ nm) acting as a depletant agent [29]. All experimental parameters are provided in Supplemental Material [30]. The resulting interaction potential, estimated from the addition of the Asakura-Oosawa [31,32] and Derjaguin-Landau-Verwey-Overbeek [33–35] potentials, is displayed in Fig. 1(a). The mobility of the active particles in the presence of blue light ($\lambda = 494/40$ nm) is characterized by their mean square displacements (MSD) [Fig. 1(b)], measured in a dilute suspension. Describing the active particles as active Brownian particles [36–38], we find a persistent time $\tau_p = 16.5 \pm 7.5$ s, independently of the light intensity, and a swimming speed U_0, which increases up to 0.57 ± 0.13 μm/s when the light intensity P reaches 154 mW/mm^2 (see also Fig. S1, Supplemental Material [30]). A significant contribution of our work is the design of this first of its kind photoswitchable model system, which successfully compromises between the need for screening the electrostatic repulsion between the colloids, while keeping a strong enough motility for the active particles.

After sedimentation, the deposited gel is left to relax for 24 h before observation. A typical illumination protocol [Fig. 2(a)] consists of 30 min recording of the gel in the absence of blue light, followed by 60 min of blue light illumination, the intensity P of which can be varied, and yet 30 min in the absence of blue light. The gel is monitored under red light ($\lambda = 647$ nm) using a confocal microscope equipped with a 40× oil objective and a scientific CMOS camera, resulting in images of size 249×173 μm^2, with a spatial resolution of 0.1625 μm/pixel, acquired at 1 frame per second (see Supplemental Material [30], Movie 1). Note that the active particles do not depart from the gel during activation. Using standard image processing techniques, we track the trajectories $\mathbf{r}_i(t)$ of the *passive* particles, from which we compute the displacement field $\Delta\mathbf{r}_i(t,\tau) = \mathbf{r}_i(t+\tau) - \mathbf{r}_i(t)$, the overlap $Q(t)$, and the square displacement averaged over the passive particles $\Delta^2_\tau(t)$:

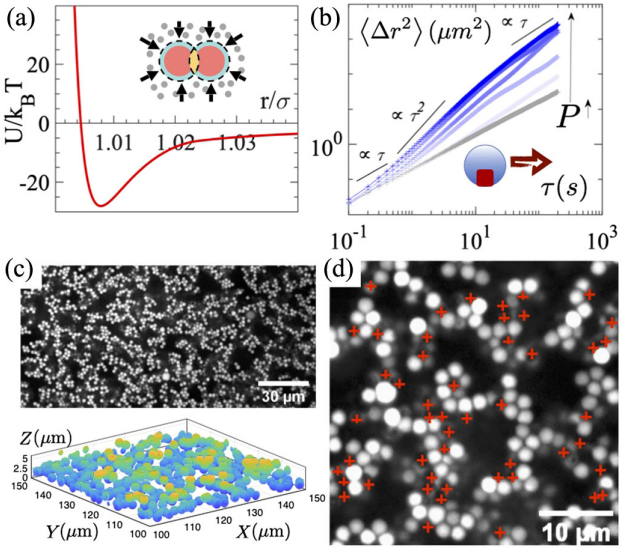

FIG. 1. Experimental system: (a) Attraction potential between the colloids composing the gel, as obtained by depletion mediated by PEO polymer. (b) Mean square displacement (MSD) of the janus particles suspended at very low density in the actual solvent used when preparing the gel, activated with different blue light intensities P, up to 154 mW/mm^2. (c) Quasi-2D gel obtained from the joint sedimentation of polystyrene colloids and janus particles in the depleting and swimming buffer: 2D projection and 3D reconstruction, color coded by height, obtained using the algorithm introduced in [39]. (d) Confocal image of the quasi-2D gel, with the janus particles marked with red crosses.

$$Q(t) = \frac{1}{N}\sum_i \exp\left(-\frac{\Delta\mathbf{r}_i^2(0,t)}{a^2}\right), \tag{1}$$

$$\Delta^2_\tau(t) = \frac{1}{N}\sum_i \Delta\mathbf{r}_i^2(t,t+\tau), \tag{2}$$

where $N \simeq 2500$ is the number of tracked passive particles and $a = \sigma/3$ is a characteristic scale of motion.

During the first passive period, the gel exhibits a slow dynamics with $\Delta^2_{100} \simeq 2 \times 10^{-3}$ μm^2, together with a slow aging, attested by the decay of $Q(t)$ [Fig. 2(b)]. When light activation is switched on ($P = 118$ mW/mm^2), a fast response of the dynamics, followed by a rapid relaxation, leads to a peak of $\Delta^2_{100} \simeq 150 \times 10^{-3}$ μm^2, before the dynamics settles to weaker values of $\Delta^2_{100} \simeq 20 \times 10^{-3}$ μm^2, still significantly larger than in the absence of light. Associated with this dynamical response, the gel reorganizes, as demonstrated by the sharp decay of Q and illustrated in Fig. 2(b), with the displacement field $\Delta\mathbf{r}_i(t, 100)$, computed around the peak of Δ^2_{100} (see also Supplemental Material, Movie 2 [30], where bursts of correlated displacements can be observed).

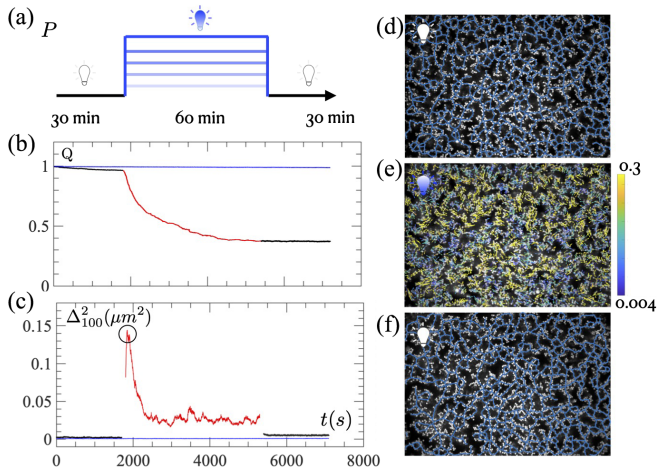

FIG. 2. Gel reconfiguration during activation: (a) Illumination protocole: 24 h after the end of sedimentation, we start recording 30 min of the dynamics of the gel, followed by 60 min of activation with blue light of various intensities and 30 min of relaxation in the absence of blue light. (b) The overlap $Q(t)$ between the gel configuration at time t and that at time $t = 0$ [see Eq. (1)]. (c) $\Delta^2_{100}(t)$, square displacements computed over $\tau = 100$ s, averaged over the passive colloids [see Eq. (2)]. (d), (f) Gel configurations before (d) and after (f) light illumination (skeleton overlaid in blue). (e) Displacement field of the passive colloids computed over $\tau = 100$ s, around the peak of Δ^2_{100}, as indicated by the black circle in panel (c), color coded by their magnitude. $P = 118$ mW/mm^2.

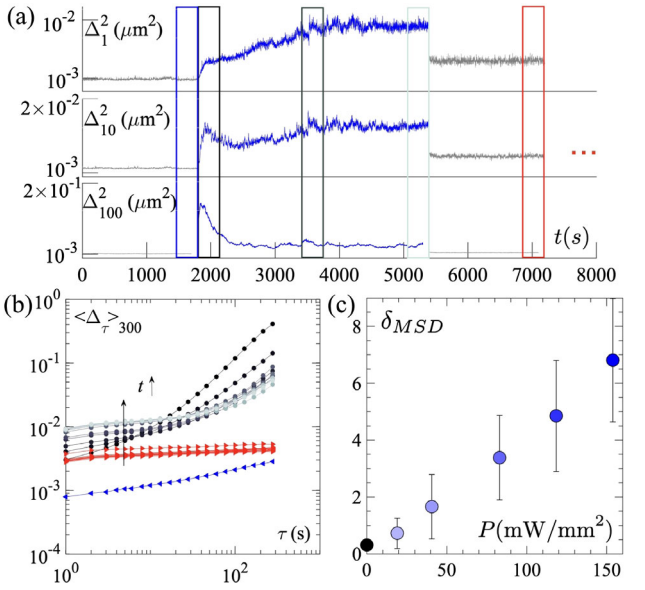

FIG. 3. Averaged dynamics: (a) Averaged square displacements $\Delta^2_1(t), \Delta^2_{10}(t), \Delta^2_{100}(t)$; (b) MSD $\langle\Delta^2_\tau\rangle_{300}$, computed at successive times indicated in panel (a) before (blue), during (gray levels), and after (red) activation; the numerous curves in red correspond to the same measurement repeated every two hours after activation, during 30 hours ($P = 118$ mW/mm^2); (c) δ_{MSD}, the relative increase of the short time ($\tau = 10$ s) MSD after activation, as a function of the light intensity during the activation period P.

When activation is switched off, we observe that (i) Q remains constant: the activation has suppressed the slow pace reorganizations, that were taking place in the passive gel. This nontrivial effect leads to a frozen gel, which thus keeps memory of the reorganization that took place during activation; and (ii) $\Delta^2_{100} \simeq 5 \times 10^{-3}$ μm^2 is larger than before activation: the gel is more motile. Figures 2(d) and 2(f) display typical gel configurations before and after illumination. The structure of the gel is certainly modified, but retains its overall integrity (see overlaid skeleton Fig. S3 in Supplemental Material [30]).

The dynamics of the gel strongly depend on the timescale τ on which it is probed [Fig. 3(a)]. While on long timescales, $\tau = 100$, the response takes the form of a sharp peak immediately following the activation, on short timescales, $\tau = 1$, the displacements essentially increase continuously during the whole activation period. As a result, the MSD, $\langle\Delta^2_\tau\rangle_{300}$, averaged over successive time windows of duration 300 s also strongly depends on the time t at which it is probed. Before activation [Fig. 3(b), blue curve], the mean dynamics is strongly subdiffusive as expected for a slowly aging gel. Just after activation [Fig. 3(b), black curve] the mean dynamics is diffusive. Later during the activation period, the gel recovers a subdiffusive dynamics although with a significantly larger amplitude [Fig. 3(b), gray curves]. The dynamical response therefore exhibits a characteristic crossover for a timescale $\tau^* \simeq 10$ s, corresponding to displacements of the order of $\Delta^* \simeq 10^{-1}$ μm. This crossover suggests that the large scale displacements $\|\Delta\mathbf{r}_i\| > \Delta^*$ triggered just after activation, contribute to a reorganization of the gel allowing for increasingly larger small scale displacements $\|\Delta\mathbf{r}_i\| < \Delta^*$ at all times. The gel after activation keeps memory of this reorganization for a long time as demonstrated by the amplitude of $\langle\Delta^2_\tau\rangle_{300}$ after activation, which remains larger than that before activation for whatever time we waited [30 h in Fig. 3(b), red curves; 11 days in Fig. S5, Supplemental Material [30]]. We also stress that $\langle\Delta^2_\tau\rangle_{300}$ after activation is flat, indicating a frozen system with fully caged particles.

Altogether the activation interrupted the slow aging of the gel and rapidly drove it into a new frozen state, which exhibits larger thermal fluctuations. This unexpected result has been confirmed, repeating the experiment over more than 80 gels, prepared in the same way, and activated with varying light intensities. The relative increase of the MSD $\delta_{\mathrm{MSD}} = (\langle\Delta_\tau\rangle_> - \langle\Delta_\tau\rangle_<)/\langle\Delta_\tau\rangle_<$, where $\langle\Delta_\tau\rangle_<$ and $\langle\Delta_\tau\rangle_>$, respectively, denote the mean square displacement computed before and after activation, is a clear growing function of the light intensity [Fig. 3(c)]. We have also checked that the above phenomenology does not rely on an alteration of the substrate nor of the PEO by the illumination (see Supplemental Material, Figs. S4, S5 [30]).

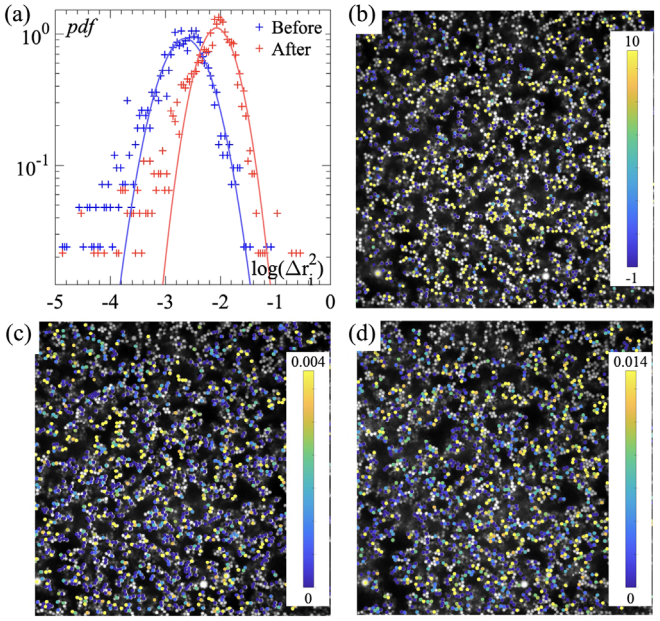

FIG. 4. Local dynamics: (a) Probability distribution of the individual square displacements $\Delta\mathbf{r}_i^2(t,10)$ before and after activation. Continuous lines indicate Gaussian distributions for comparison. (b) Spatial distribution of δ_{MSD}. (c),(d) Spatial distribution of $\Delta\mathbf{r}_i^2(t,100)$, respectively, before and after activation. The color bar ranges are scaled to 2 times the average value.

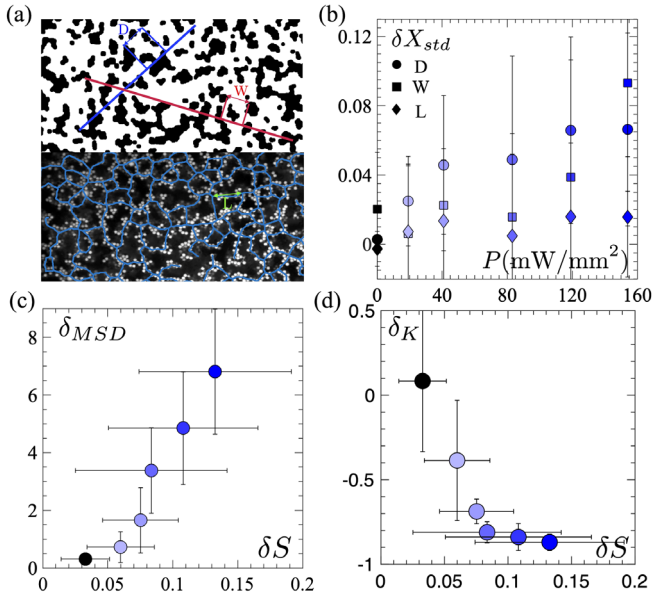

FIG. 5. Gel structure: (a) Top: Binary density field and a sample of chord lengths defining the strands width W and the pores size D. Bottom: Gel skeleton as obtained by morphological analysis of the binary density field (see Supplemental Material [30]); the green arrow indicates the length L of a gel strand. (b) Relative variation of the standard deviation of the pores size δD_{std}, the strand width δW_{std}, and the link length δL_{std} with increasing light activation. (c) Correlation between the relative increase of the short time mean square displacement δ_{MSD} and the structural change δS. (d) Correlation between the relative decrease of the effective stiffness of the strand δ_K and the structural change δS.

Figure 4 demonstrates that the above phenomenology homogeneously takes place in the gel. The probability distributions of $\Delta\mathbf{r}_i^2(t,10)$ [Fig. 4(a)], before and after activation are very similar and essentially simply shifted to larger values. Their spatial distribution is homogeneous, both before and after activation, even a bit more homogeneous following activation [Figs. 4(c) and 4(d)]. Finally, δ_{MSD}, when computed for individual particles is also homogeneously distributed in space [Fig. 4(b)].

As stated above, there is no obvious direct visual evidence of a modification of the structure, which could simply explain the observed dynamical changes. The pair correlation functions before and after activation are essentially identical (see Fig. S2, Supplemental Material [30]). We thus further characterize the gel structure by performing a morphological image analysis, which consists of approximating the instantaneous density field by a binary image, from which we extract a set Xq of structural parameters: the width of the gel strands, $X1 = W$, and the size of the gel pores, $X2 = D$. We further skeletonize the binary image [40], to extract the strands lengths, $X3 = L$ [Fig. 5(a) and Supplemental Material, Fig. S3(a) [30]]. We then compute their spatiotemporal average $\bar{X}q$ and standard deviation Xq_{std} before ($\langle$) and after ($\rangle$) activation, for each gel. We denote $\delta\bar{X}q = (\bar{X}q_{>} - \bar{X}q_{<})/\bar{X}q_{<}$ and $\delta Xq_{\mathrm{std}} = (Xq_{\mathrm{std},>} - Xq_{\mathrm{std},<})/Xq_{\mathrm{std},<}$ the variation of these statistical descriptors of the gel structure across activation. The average strand width and the pore size increase by a few percent, the variation being larger with stronger activation, while the strand length remains essentially unchanged [see Supplemental Material, Fig. S3(b) [30]]. These admittedly small variations suggest a weak coarsening of the gel structure. The evolution of the gel structure appears more clearly on the standard deviations, which increase more systematically, indicating a more heterogeneous structure after activation [Fig. 5(b)]. Defining $\delta S = (\sum_q \delta Xq_{\mathrm{std}}^2)^{1/2}$, a parameter quantifying the overall relative variation of the structure heterogeneity induced by the activation, we observe that the dynamical change correlates very well with it [Fig. 5(c)]: the more the structure heterogeneity has increased, the more the short time mean square displacement has increased. Associated with this increase of structural heterogeneity, we also observe in Fig. 5(d) a decreased effective stiffness K of the strands. The latter is estimated from the thermal fluctuations of the pair distance as the quadratic interpolation of the logarithm of their steady state distribution [41] (see also Supplemental Material [30]). Note that in the absence of activation, $\delta_K > 0$, the effective stiffness actually increases.

In discussing the above results, it is useful, following [10], to compute the strength of the swim force $F_s = \zeta U_0$ relative to the attractive force scale $F_a = E_0/2R_g$, where E_0

is the depth of the attractive potential and R_g is the interaction range given by the gyration radius of the PEO. We find that for the maximal light intensity $F_s/F_a \simeq 10^{-2}$ confirming that the active particles cannot individually break bonds. However, there are also two active energy scales to consider: $E_s = F_s\sigma \simeq 10k_BT$ and $E_p = F_s l_p \simeq 100k_BT$, where $l_p = U_0\tau_p$ is the active persistence length. These energy scales are comparable to or larger than $E_0 \simeq 25k_BT$, indicating that the collective contribution of a few active particles can easily produce local rearrangements. Note that activity not only acts as an effective hot temperature; it can also activate elasticity driven relaxation, which are central to the complex time-dependence signature of aging in gels [42].

Our observations during the activation period compare well, and extend to a higher level of activity, those of Solomon and collaborators [22–24]: activity increases the dynamics and decreases the gel stiffness, while hardly modifying the structure of the gel. An important difference, though, is that we prepare the gel in a passive state, before the response to activity is studied. From that point of view, it is of interest to compare our result to that of the response to a global shear [43–45], in the spirit of the theoretical link made between both [46]. In both cases the gel becomes more heterogeneous, with larger voids, locally compacted regions, and rather small changes in the short range structure. The gel also becomes softer. This last observation supports recent claims about the role of structural heterogeneities in the softness of gels [47–50].

Altogether, we present a new pathway, using switchable local activation, toward a fast synthesis of stable colloidal gels with tunable softness. The present system has a number of tunable parameters such as the packing fraction or the depletion attraction, opening room for optimization. Extending the present work to 3D gels is an interesting route, which will, however, pose a material science challenge for adapting this heterogenous system for confocal microscopy (see Supplemental Material [30]). On the theoretical side, one would like to identify the type of state the gel has reached, and understand if and how they differ from their equilibrium counterparts.

We thank Laura Rossi, from TU-Delft for providing us with the Hematite-TPM particles. We thank Patrick C. Royall and Emanuela del Gado for inspiring discussions. M. W. acknowledges support from Chinese Scientific Council (N° 201806120044).

[1] G. M. Whitesides and B. Grzybowski, Science **295**, 2418 (2002).
[2] S. Sacanna, L. Rossi, and D. J. Pine, J. Am. Chem. Soc. **134**, 6112 (2012).
[3] M. Y. Ben Zion, X. He, C. C. Maass, R. Sha, N. C. Seeman, and P. M. Chaikin, Science **358**, 633 (2017).
[4] C. L. Kennedy, D. Sayasilpi, P. Schall, and J.-M. Meijer, J. Phys. Condens. Matter **34**, 214005 (2022).
[5] R. Ni, M. A. C. Stuart, M. Dijkstra, and P. G. Bolhuis, Soft Matter **10**, 6609 (2014).
[6] K. Dietrich, G. Volpe, M. N. Sulaiman, D. Renggli, I. Buttinoni, and L. Isa, Phys. Rev. Lett. **120**, 268004 (2018).
[7] S. Mallory, M. Bowers, and A. Cacciuto, J. Chem. Phys. **153**, 084901 (2020).
[8] B. Van Der Meer, L. Filion, and M. Dijkstra, Soft Matter **12**, 3406 (2016).
[9] D. P. Singh, U. Choudhury, P. Fischer, and A. G. Mark, Adv. Mater. **29**, 1701328 (2017).
[10] A. K. Omar, Y. Wu, Z.-G. Wang, and J. F. Brady, ACS Nano **13**, 560 (2018).
[11] S. Ramananarivo, E. Ducrot, and J. Palacci, Nat. Commun. **10**, 3380 (2019).
[12] L. M. Janssen, J. Phys. Condens. Matter **31**, 503002 (2019).
[13] G. H. Koenderink, Z. Dogic, F. Nakamura, P. M. Bendix, F. C. MacKintosh, J. H. Hartwig, T. P. Stossel, and D. A. Weitz, Proc. Natl. Acad. Sci. U.S.A. **106**, 15192 (2009).
[14] T. Sanchez, D. Welch, D. Nicastro, and Z. Dogic, Science **333**, 456 (2011).
[15] T. Sanchez, D. T. Chen, S. J. DeCamp, M. Heymann, and Z. Dogic, Nature (London) **491**, 431 (2012).
[16] J. Berezney, B. L. Goode, S. Fraden, and Z. Dogic, Proc. Natl. Acad. Sci. U.S.A. **119**, e2115895119 (2022).
[17] M. Gardel, J. H. Shin, F. MacKintosh, L. Mahadevan, P. Matsudaira, and D. A. Weitz, Science **304**, 1301 (2004).
[18] C. Storm, J. J. Pastore, F. C. MacKintosh, T. C. Lubensky, and P. A. Janmey, Nature (London) **435**, 191 (2005).
[19] D. Mizuno, C. Tardin, C. F. Schmidt, and F. C. MacKintosh, Science **315**, 370 (2007).
[20] P. Ronceray, C. P. Broedersz, and M. Lenz, Proc. Natl. Acad. Sci. U.S.A. **113**, 2827 (2016).
[21] D. Goldstein, S. Ramaswamy, and B. Chakraborty, Soft Matter **15**, 3520 (2019).
[22] M. E. Szakasits, W. Zhang, and M. J. Solomon, Phys. Rev. Lett. **119**, 058001 (2017).
[23] M. E. Szakasits, K. T. Saud, X. Mao, and M. J. Solomon, Soft Matter **15**, 8012 (2019).
[24] K. T. Saud, M. Ganesan, and M. J. Solomon, J. Rheol. **65**, 225 (2021).
[25] J. Palacci, S. Sacanna, A. P. Steinberg, D. J. Pine, and P. M. Chaikin, Science **339**, 936 (2013).
[26] T. Sugimoto, M. M. Khan, and A. Muramatsu, Colloids Surf. A **70**, 167 (1993).
[27] S. Sacanna, L. Rossi, and D. J. Pine, J. Am. Chem. Soc. **134**, 6112 (2012).
[28] J. Palacci, S. Sacanna, S.-H. Kim, G.-R. Yi, D. J. Pine, and P. M. Chaikin, Phil. Trans. R. Soc. A **372**, 20130372 (2014).
[29] K. Devanand and J. Selser, Macromolecules **24**, 5943 (1991).
[30] See Supplemental Material at http://link.aps.org/supplemental/10.1103/PhysRevLett.131.018301 for detailed experimental protocoles, and how to access additional movies.
[31] S. Asakura and F. Oosawa, J. Chem. Phys. **22**, 1255 (1954).
[32] A. Vrij, in *Colloid and Surface Science* (Elsevier, New York, 1977), pp. 471–483.
[33] B. Derjaguin, Prog. Surf. Sci. **43**, 1 (1993).
[34] B. V. Derjaguin, Acta Phys. Chim. URSS **14**, 633 (1941).

[35] E. J. W. Verwey, J. Phys. Chem. **51**, 631 (1947).
[36] K. Franke and H. Gruler, Eur. Biophys. J. **18**, 334 (1990).
[37] J. R. Howse, R. A. L. Jones, A. J. Ryan, T. Gough, R. Vafabakhsh, and R. Golestanian, Phys. Rev. Lett. **99**, 048102 (2007).
[38] G. E. Uhlenbeck and L. S. Ornstein, Phys. Rev. **36**, 823 (1930).
[39] M. Leocmach and H. Tanaka, Soft Matter **9**, 1447 (2013).
[40] T.-C. Lee, R. L. Kashyap, and C.-N. Chu, CVGIP: Graphical Models Image Process. **56**, 462 (1994).
[41] A. Dinsmore and D. Weitz, J. Phys. Condens. Matter **14**, 7581 (2002).
[42] M. Bouzid, J. Colombo, L. V. Barbosa, and E. Del Gado, Nat. Commun. **8**, 15846 (2017).
[43] K. Masschaele, J. Fransaer, and J. Vermant, J. Rheol. **53**, 1437 (2009).
[44] K. Masschaele, J. Fransaer, and J. Vermant, Soft Matter **7**, 7717 (2011).
[45] H. Hoekstra, J. Vermant, J. Mewis, and G. Fuller, Langmuir **19**, 9134 (2003).
[46] P. K. Morse, S. Roy, E. Agoritsas, E. Stanifer, E. I. Corwin, and M. L. Manning, Proc. Natl. Acad. Sci. U.S.A. **118**, e2019909118 (2021).
[47] E. Del Gado and W. Kob, Phys. Rev. Lett. **98**, 028303 (2007).
[48] J. Colombo, A. Widmer-Cooper, and E. Del Gado, Phys. Rev. Lett. **110**, 198301 (2013).
[49] D. Z. Rocklin, L. Hsiao, M. Szakasits, M. J. Solomon, and X. Mao, Soft Matter **17**, 6929 (2021).
[50] M. Bantawa, B. Keshavarz, M. Geri, M. Bouzid, T. Divoux, G. H. McKinley, and E. Del Gado, Nat. Phys. 1 (2023).